Reorganization of Cingulate Cortex in Alzheimer's Disease: Neuron Loss, Neuritic Plaques, and Muscarinic Receptor Binding

Brent A. Vogt,[1] Peter B. Crino,[2] and Leslie J. Vogt[1]

Department of Physiology and Pharmacology, Bowman Gray School of Medicine, Wake Forest University, Winston-Salem, North Carolina 27103 and [2] Department of Neurology, Hospital of the University of Pennsylvania, Philadelphia, Pennsylvania 19104

Pathology related to dementia of the Alzheimer type (DAT) develops later in cingulate cortex than in medial temporal areas. Therefore, end-stage cases have earlier forms of pathology in cingulate cortex, and postmortem studies of this region may provide a window on processes that temporal cortices pass through decades before death. Five classes of DAT have been described on the basis of neuron degeneration and receptor binding in posterior cingulate cortex. The present study assessed binding of ^{3}H-oxotremorine-M with pirenzepine (OXO-M/PZ), a protocol for presynaptic muscarinic receptors, and thioflavin S–stained neuritic plaques (NPs) in cingulate area 23a in 12 DAT cases distributed over four classes of pathology and in nine age-matched control cases. OXO-M/PZ binding was significantly elevated in layers I, II, IV, and VI of all DAT cases and was very high in layer V compared to control cases. Almost 75% of the layer Va increase was due to binding in classes 2 and 3, while classes 1 and 4 were least affected. In class 3 cases, neuron density in layer Va was inversely correlated with OXO-M/PZ binding ($r = -0.98$) and primitive NP densities ($r = -0.93$). The close association between neuron densities and presynaptic muscarinic ligand binding in some classes confirms that there are independent classes of DAT. The high and inverse correlations between cortical pathology and ligand binding in class 3 cases suggest that there is a progression in class 3 pathology. Finally, elevated OXO-M/PZ binding and a report of increased choline uptake suggest that cholinergic axons sprout in DAT, and this sprouting may be associated with a progressive loss of postsynaptic elements.

One feature of the pathology related to dementia of the Alzheimer type (DAT) is degeneration of cholinergic basal forebrain neurons (Whitehouse et al., 1982; Arendt et al., 1983), and reductions in cortical activity of the ACh synthetic enzyme ChAT (Rossor et al., 1982; Procter et al., 1988). A paradox of DAT research, however, has been a lack of consistent findings relating the cholinergic deafferentation lesion with cortical muscarinic ACh receptors. Neurons in the basal forebrain synthesize m2 receptors (Buckley et al., 1988) and express presynaptic receptor binding on their cortical terminals (Mash et al., 1985). Although Mash et al. (1985) observed reduced muscarinic ligand binding and ChAT activity in DAT neocortex, there are reports of elevated binding of the nonselective muscarinic antagonist quinuclidinyl benzilate in cases with significantly reduced ChAT activity (Nordberg and Winblad, 1986; Danielsson et al., 1988; Giacobini et al., 1989). Furthermore, Slotkin et al. (1990) observed increased choline uptake into synaptosomes that had reduced ChAT activity, shrunken neurons can persist in the nucleus basalis of Meynert in DAT (Pearson et al., 1983), and Henke and Lang (1983) reported that four of nine DAT cases had significantly elevated ChAT activity in layers I–IV of cingulate cortex. One explanation for elevated muscarinic receptor binding, choline uptake, and ChAT activity is sprouting of cholinergic axons that project from the basal forebrain to the cerebral cortex.

A number of variables contribute to the different outcomes of ligand binding studies of DAT These include the use of antagonists that bind to all or a few of the muscarinic receptor subtypes, receptors on pre- and postsynaptic processes, and a wide variation in DAT pathology in neocortex. In terms of muscarinic receptor binding, the m1, m3, and m4 receptors are expressed by cortical neurons while m2 receptors are expressed by basal forebrain and anterior thalamic neurons (Buckley et al., 1988). There is overlap in ligand binding to these receptors; for example, pirenzepine has the highest affinity for m1 and m4 receptors (Dörje et al., 1991), and AF-DX 116 has highest affinity for m2 receptors but also binds to m4 receptors (Buckley et al., 1989). We have used pirenzepine to increase the specificity of ligands for presynaptic m2 receptors, and since anterior thalamic neurons synthesize m2 but not m4 receptors, binding specificity has been verified with thalamic lesions

Cerebral Cortex Nov/Dec 1992,2:526–535; 1047–3211/92/$4.00

Downloaded from http://cercor.oxfordjournals.org/ at Boston University on June 28, 2015

(Vogt and Burns, 1988; Vogt et al., 1992). Between 70% and 80% of cingulate layer Ia binding of AF-DX 116 or oxotremorine-M with unlabeled pirenzepine (OXO-M/PZ) can be abolished by thalamic lesions. Thus, both basal forebrain and thalamic afferents to cingulate cortex have presynaptic m2 receptors that can be assessed with ligand binding protocols. Furthermore, since the limbic thalamic nuclei express pathology in DAT (Braak and Braak, 1991a), both of these inputs to cingulate cortex may be impaired in DAT and need to be considered in relation to presynaptic muscarinic receptor binding.

Another critical variable in ligand binding studies of DAT is that the underlying neocortical pathology is not uniform. In contrast to areas like the hippocampus and entorhinal cortex where there is a consistent pathology in end-stage cases, many neocortical areas express a wide range of damage; in other words, pathophysiological processes have not necessarily reached completion in these regions in end-stage cases. For example, Brun and Englund (1981) observed that neuron degeneration was most variable in posterior cingulate cortex, with a range from no loss to 80% loss of neurons. They proposed that these differences could be accounted for by a graded series of changes in neuron degeneration. A subsequent study, however, analyzed neuron degeneration in each layer of area 23 of posterior cingulate cortex and showed that there was not a simple progression from little to severe neuron loss (Vogt et al., 1990) Rather, the cases could be classified into five classes based on the layer and extent of neuron degeneration: class 1 had no neuron loss, class 2 had greatest losses in layers II and/or III, class 3 had losses mainly in layer IV, class 4 had losses primarily in layers V and/or VI, and class 5 had severe degeneration that was not limited to a few layers. Furthermore, ligand binding to $GABA_A$ and β adrenoceptors was reduced or elevated, respectively, according to the class based on neuron degeneration, while there were few or no changes in pirenzepine binding to muscarinic receptors in classes of DAT (Vogt et al., 1991). In view of this latter finding, reports of elevated quinuclidinyl benzilate binding may reflect changes in binding to m2 receptors. This classification scheme provides a unique approach to evaluate variations in ligand binding in relationship to neuron degeneration and classical measures of DAT pathology including the deposition of neurofibrillary tangles (NFTs) and neuritic plaques (NPs).

The present study was undertaken because preliminary observations showed that, although pirenzepine binding was stable in class 3 DAT cases, there was a massive increase in binding of oxotremorine-M in these same cases. Thus, oxotremorine-M binding was evaluated for each of four classes of DAT, and the binding was related to the underlying neuron densities, as well as the distribution, densities, and stages of formation of NPs and NFTs. The outcome of this analysis is that there is a strong and inverse relationship between neuron degeneration and oxotremorine-M binding in layer V of posterior cingulate cortex. Furthermore, within class 3, there is a gradation of neuron degeneration and the number of NPs such that cases with greatest neuron degeneration in layer Va have the fewest NPs. These relationships can be understood in the framework of disease progression within a single class of DAT, and they have implications for understanding the pathophysiology in preclinical states of DAT including changes that likely occur in medial temporal cortices long before death.

Materials and Methods

Case Material

Twelve cases for this study were diagnosed as DAT based on clinical and neuropathological criteria (McKhann et al , 1984). The average age at death for these and nine neurologically intact, age-matched control cases is presented in Table 1. Other information relating to estimations of age at disease onset and length of disease, brain weights, and postmortem intervals have been reported for these cases (Vogt et al., 1991). The drug histories of these patients were surveyed for compounds with CNS actions that were administered for 1 or more weeks during the 6 months prior to death. Five of the 12 DAT cases received compounds that have antagonist actions at muscarinic acetylcholine receptors including atropine, chlorpromazine, diphenhydramine, loxapine, and metoclopramide. Three DAT patients received benzodiazepines including oxazepam or temazepam, and two received morphine. Of the nine control cases, six received morphine; three, benzodiazepine agonists (triazolam, oxazepam, or alprazolam); two, the β adrenoceptor antagonist atenolol; and one, chlorpromazine.

Neuropathological Assessment

The methods for neuropathological assessment have been previously reported (Vogt et al., 1990). Blocks of posterior cingulate cortex including the corpus callosum (see Fig. 2) were dissected and frozen to −70°C, or transverse slabs 1–2 cm thick were frozen to this temperature and the cingulate cortex removed without intermediate thawing. Sections were cut on a cryostat for ligand binding at a 16 μm thickness, and those for thionin and thioflavin S staining were cut at a 48 μm thickness.

The cases were classified according to neuron loss in the following manner. The perikarya of thionin-stained neurons in area 23a that had nucleoli were drawn with a drawing tube attachment to a light microscope at a final magnification of 650×. Strips of perikarya 160 μm in width were drawn extending from layer II to the white matter. The mean number of perikarya in each layer was calculated for two sections, and this mean was compared to a mean for the control cases. The layer with the largest percentage reduction in neuron density when compared to the control mean was used to classify each DAT case. This relative measure was originally used so that material prepared in different ways could be combined with-

Downloaded from http://cercor.oxfordjournals.org/ at Boston University on June 28, 2015

Table 1
Summary of case data

	Control (n = 9)	All DAT (n = 12)	Class 1 (n = 3)	Class 2 (n = 3)	Class 3 (n = 4)	Class 4 (n = 2)
Age at Death						
(Years ± SEM)	68 ± 3	70 ± 2	71 ± 4	72 ± 6	69 ± 2	67 ± 0
Area 23a neuron density (perikarya ± SEM/160-μm-wide layer)						
IIIa,b	45 ± 6	35 ± 4	46 ± 7	19 ± 2*	36 ± 6	38 ± 5
IIIc	34 ± 4	31 ± 4	41 ± 6	19 ± 3	31 ± 7	35 ± 9
IV	19 ± 2	14 ± 3	27 ± 6	12 ± 2	8 ± 1**	12 ± 7
Va	39 ± 3	28 ± 3**	41 ± 3	29 ± 4	24 ± 2**	14 ± 6*
Area 23a NP (mean ± SEM)						
Primitive	—	49 ± 16	29 ± 9	114 ± 40	36 ± 16	9 ± 0
Mature	—	86 ± 23	75 ± 12	128 ± 58	102 ± 50	25 ± 13
Compact	—	20 ± 6	15 ± 9	9 ± 6	35 ± 13	17 ± 15
White Matter	—	9 ± 4	8 ± 4	2 ± 1	20 ± 10	3 ± 3
Area 23a NFT (mean ± SEM)						
III	—	127 ± 57	65 ± 16	198 ± 149	169 ± 165	29 ± 5
IV	—	68 ± 26	34 ± 15	121 ± 99	56 ± 36	55 ± 40
V	—	111 ± 32	119 ± 25	202 ± 108	74 ± 52	35 ± 2

*$p \leq 0.01$; **$p \leq 0.05$, in comparison to control values.

out correcting for differences in tissue shrinkage. Cases in class 1 had no evidence of neuron degeneration, those in class 2 had greatest percentage losses in layers II and/or III, those in class 3 had greatest losses in layer IV, while those in class 4 had greatest degeneration in layers V and/or VI. When compared to control cases with protected t tests for multiple comparisons, the absolute numbers of neurons in the layer with greatest percentage changes were also significantly reduced.

Sections adjacent to the Nissl-stained sections were stained with thioflavin S (Schwartz et al., 1964) and were analyzed for the distribution of neurofibrillary tangles (NFTs) and neuritic plaques (NPs) with an epifluorescence microscope. The distribution of these structures was plotted with an x–y plotter attached to the microscope stage, and the total number of each pathological marker was calculated for area 23a. The NPs were further distinguished according to the "stage of maturation" (Wisniewski and Terry, 1973): primitive, mature (i.e., classic), and compact. In order to increase the chances that mature plaques that were cut off-center from the dense core were not counted as primitive, NPs were only counted as primitive when they were of the same diameter as mature NPs, that is, diameters >25 μm. The densities of NFTs in each layer were estimated based on the laminar cytoarchitecture of area 23a in adjacent Nissl-stained sections.

Ligand Binding and Autoradiographic Protocols

Unlabeled pirenzepine was kindly provided by Boehringer Ingelheim, Ltd. Radiolabeled ligands were purchased from New England Nuclear–DuPont and included ^{3}H-oxotremorine-M (specific activity, 85.1 Ci/mM) and ^{3}H-AF-DX 116 (specific activity, 59.8 Ci/mM). All incubation buffers were at pH 7.4. For the oxotremorine-M procedure, sections were incubated in 5 nM ^{3}H-oxotremorine-M in 20 mM HEPES Tris buffer with 10 mM Mg^{2+} and 50 nM pirenzepine for 30 min at 25°C. This was followed by two buffer washes at 4°C for 2 min each and one 2 min distilled water wash and rapid air drying. Nonspecific binding was determined with 1 μM atropine in a parallel series of sections. Lower concentrations of oxotremorine-M were also used including 1 nM and 0.1 nM, since these concentrations were more effective in rat studies for labeling presynaptic m2 receptors (Vogt and Burns, 1988; Vogt et al., 1992). OXO-M/PZ binding at these concentrations in human, however, produced very little specific binding, was relatively homogeneous throughout the cortical thickness, and was not elevated in any classes of DAT. Finally, since Scatchard analysis was not performed in these studies, it is not known whether the elevated binding of OXO-M/PZ was due to a change in the affinity or density of muscarinic receptors.

The procedure for AF-DX 116 binding included preincubation of the sections in 50 mM Na/KPO_4 buffer for 30 min at 25°C. Incubation was in the same buffer with 5 nM ^{3}H-AF-DX 116 for 30 min at 25°C followed by a 3 min wash in buffer at 4°C, a 1 min wash in distilled water at 4°C, and rapid air drying. Nonspecific binding was assessed with 1 μM atropine in a parallel series of sections.

Autoradiographs were prepared according to the method of Young and Kuhar (1979) so that binding could be assessed directly in the underlying cortical layers. Coverslips were acid cleaned and dipped in Kodak NTB-2 nuclear tract emulsion. The dried coverslips were attached to slides with cyanoacrylate and exposed in the dark at −20°C for 3–4 months. All autoradiographs were developed in Kodak D-19 without hardener, fixed in Kodak Rapid Fixer, and counterstained with thionin. It should be noted that all cases were prepared at the same time for these studies so that the autoradiograph exposure and develop-

Downloaded from http://cercor.oxfordjournals.org/ at Boston University on June 28, 2015

ment procedures were exactly the same for all brains Thus, the absolute differences in grain densities are quantitatively meaningful and correction factors for standardizing different series of autoradiographs were not needed.

Quantification of Autoradiographs and Data Analysis

The dorsoventral limits of area 23a are shown schematically below (see Fig. 2). Each of nine layers were determined using bright-field illumination, and then dark-field illumination was used to image single grains with a computerized image analysis system (Image Technology Model 1000, Donsanto Corp, Natick, MA). Grains were counted per 2500 μm^2 of a cortical layer in three nonadjacent sections incubated without a blocker and in two sections in which atropine was present. The readings were visually corrected for miscounts due to overlapping grains (i.e., the image analyzer could not detect overlapping grains) and then averaged. Nonspecific binding in the atropine series was subtracted from total binding to determine specific binding. The mean specific binding was calculated for each layer of each case. The means ± SEM reported here are for all control cases, for all DAT cases, and for each class of DAT cases.

Specific binding for control and all DAT cases was compared for each layer with a one-way analysis of variance. Subsequently, the DAT cases were separated into classes, and the binding was calculated for each class. Protected *t* tests for multiple comparisons (Couch, 1982; software produced for IBM-AT computers by Dynamic Microsystems, Inc., Silver Springs, MD) were performed. The Pearson product moment correlation coefficient was used to determine the level to which ligand binding was correlated with neuron densities and relationships between neuron densities and neuritic plaques. Linear regressions were also used to estimate the functions that would best fit these relationships when significant ANOVA *F* values were observed.

Results

Neuron Density, NPs, and NFTs

Neuron densities have been reported for these control and DAT cases (Vogt et al., 1991); however, the densities for layers III, IV, and Va are repeated in Table 1 because of their particular relevance to the ligand binding studies. Class 1 had no neuron losses. Greatest percentage and absolute losses in layer IIIa,b of the class 2 cases were statistically significant. Class 3 cases had the greatest loss of neurons in layer IV. Notice also that there was a significant reduction in neuron density in layer Va in the class 3 cases. Class 4 cases were defined by the high proportion of neurons that were lost in deep layers, and this is shown by the significant reduction of neurons in layer Va, although they also had significant losses in layer VI.

There were no thioflavin S–stained NPs in cingulate cortex in the control cases. Although a wide range of variation in the densities of NPs in each class have been reported for a larger sample of DAT cases (Vogt et al., 1990), the possibility was considered that neuron densities might be significantly related to the densities of NPs in area 23a. In most of these cases there was a homogeneous distribution of NPs (i.e., they were not usually localized to a particular layer) and so NPs were counted in all of area 23a rather than in individual layers. As shown in Table 1, there were low numbers of compact and white matter NPs in each class and the number of primitive and mature NPs were low in class 4; therefore, they will not be considered further. In spite of a high degree of variation, the densities of both primitive and mature NPs were as follows: class 2 > class 3 > class 1

Neurons in layers IIIa,b, IIIc, IV, and Va were evaluated as a function of total NPs for DAT cases via correlation and linear regression analyses. There were no significant relationships between these factors when all DAT cases were considered as a group, or when cases in classes 1–3, which showed increases in layer Va OXO-M/PZ binding as discussed below, were considered as a group. There was, however, a significant correlation between layer Va neuron density and primitive NPs for cases in class 3 ($r = -0.93$; $F = 26.6$; $p = 0.036$). The two cases with fewest neurons in layer Va (20.5 ± 1 5) had few primitive NPs (7.5 ± 3.5), while the two cases with most neurons in layer Va (27 ± 1.0) had most primitive NPs (65 ± 2.5) A photograph of the primitive NPs and NFTs in layer IV in one of the latter two cases is shown in Figure 1. It should be noted that there were no significant relationships between neuron densities in layer IV of the class 3 cases and NPs because there were essentially no neurons in layer IV of these cases. Finally, there was no significant correlation between neuron densities in layer IIIa,b and NPs in area 23a for all DAT cases nor for any class of DAT.

There was a wide range of NFTs in layers III, IV and V of area 23a (Table 1). Layers II and VI are not presented because alterations of neuron densities in these layers did not have an impact on the primary classification of the DAT cases. There were no significant correlations between the densities of NFTs and neuron densities in layers IIIa,b, IV or Va Although the class 3 case shown in Figure 1 had a high density of NFTs in layer IV, the most that can be said for the class 3 cases is that the two cases with fewest primitive NPs also had fewest NFTs in layer IV (5.5 ± 5.5) and the two cases with most primitive NPs had most NFTs in layer IV (112 ± 14).

Oxotremorine-M Binding

In control cases specific binding of ^{3}H-oxotremorine-M with 50 nM pirenzepine (OXO-M/PZ) in area 23a was highest in layer IIIc as shown in Figure 2. This binding, however, was very close to that in layers IIIa,b, IV, and Va. Moderate levels of binding were in layers Ic, II, and Vb, and low levels of binding were in layers Ia and VI.

Binding of OXO-M/PZ in all DAT cases was significantly elevated over that for control cases in layers I, II, IV, V and VI, and the largest increase was in

Downloaded from http://cercor.oxfordjournals.org/ at Boston University on June 28, 2015

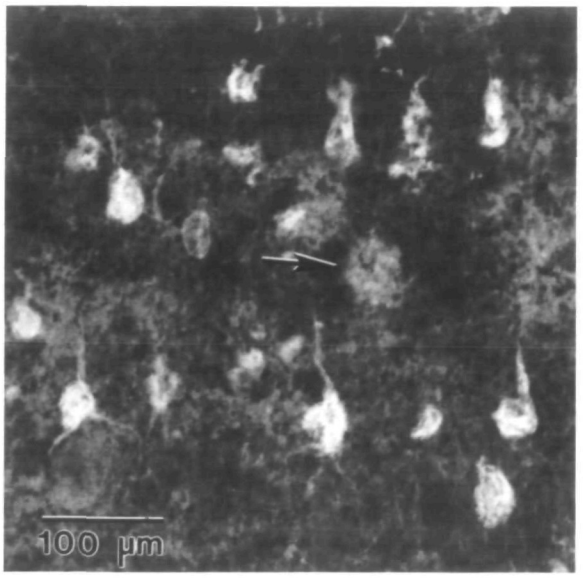

Figure 1. Photomicrograph of thioflavin S–stained preparation of a class 3 case to show primitive NPs (*arrow*) and NFTs in the small pyramidal neurons in layer IV.

layer Va (Table 2, Fig. 2). Most of the elevated binding observed in all DAT cases was due to that in classes 2 and 3, while there was very little change over that in control cases for classes 1 and 4 (Table 2). In layer Va, for example, class 3 cases accounted for almost half of the increase, while class 2 cases accounted for about 25% of the increase. Examples of elevated OXO-M/PZ binding in layer Va in two class 3 DAT cases are compared with binding in a control case in Figure 3. These photographs are of total binding, since specific binding is calculated from area densities of total and nonspecific binding from parallel series. It should also be noted that the section from the control case (Fig. 3*E*) was on the same slide as the section from the class 3 case (Fig. 3*B*), and each contributed to the same autoradiograph. Therefore, the quantitative differences in the grain densities between these two sections are particularly noteworthy.

Elevated OXO-M/PZ binding was not unique to area 23a, since it was present in each of the three cytoarchitectural subdivisions of area 23. Also, in one case the cingulate cortices of both hemispheres were included in the same preparation and in this case elevated binding was present in both hemispheres. Finally, nonspecific binding in these cases was relatively low. For example, nonspecific binding as a percentage of total binding in layer Va of class 3 cases was 9.8 ± 1.4%.

The greatest elevation in OXO-M/PZ binding occurred in layer Va of classes 2 and 3. Since layer Va also had a wide range in neuron degeneration, it was

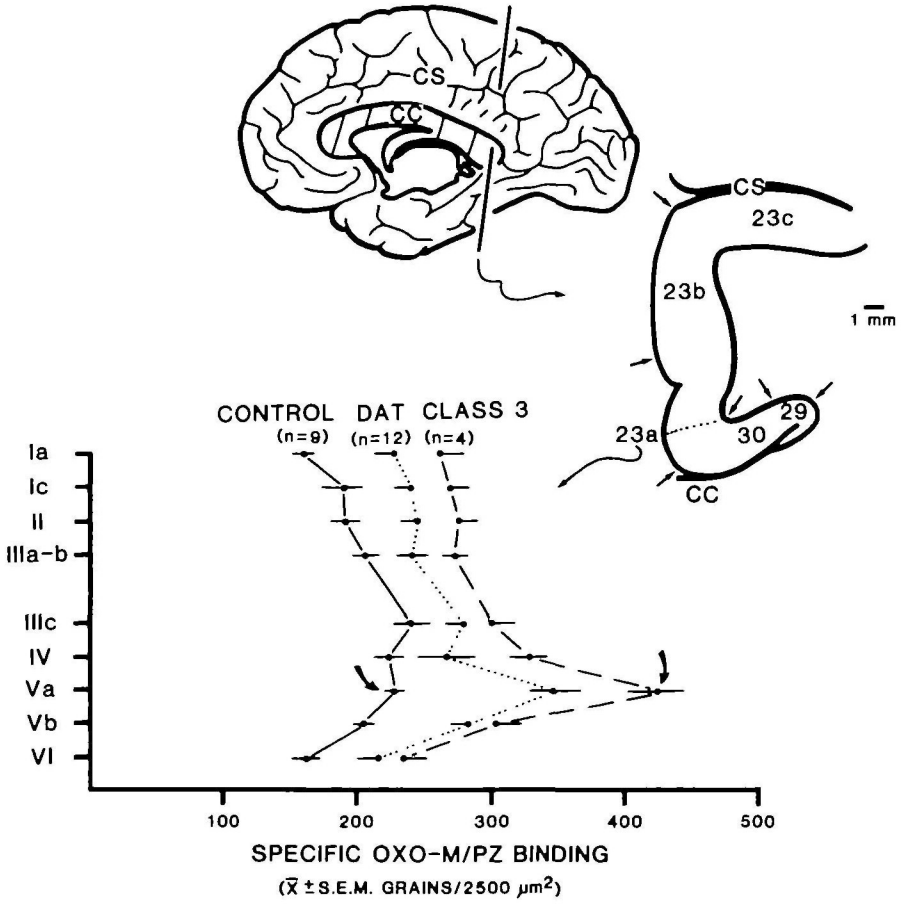

Figure 2. Transverse sections were removed from posterior cingulate cortex as shown on the medial view of the hemisphere (*CS*, cingulate sulcus; *CC*, corpus callosum; *arrows* indicate borders between areas). Quantitative assessments of OXO-M/PZ binding were made for each layer of area 23a for control, all DAT, and each class of DAT as shown for class 3 in the graph. The greatest increase in OXO-M/PZ binding was in layer Va of class 3 cases when compared to control cases, and this is indicated in the *graph* with the *arrows*.

Downloaded from http://cercor.oxfordjournals.org/ at Boston University on June 28, 2015

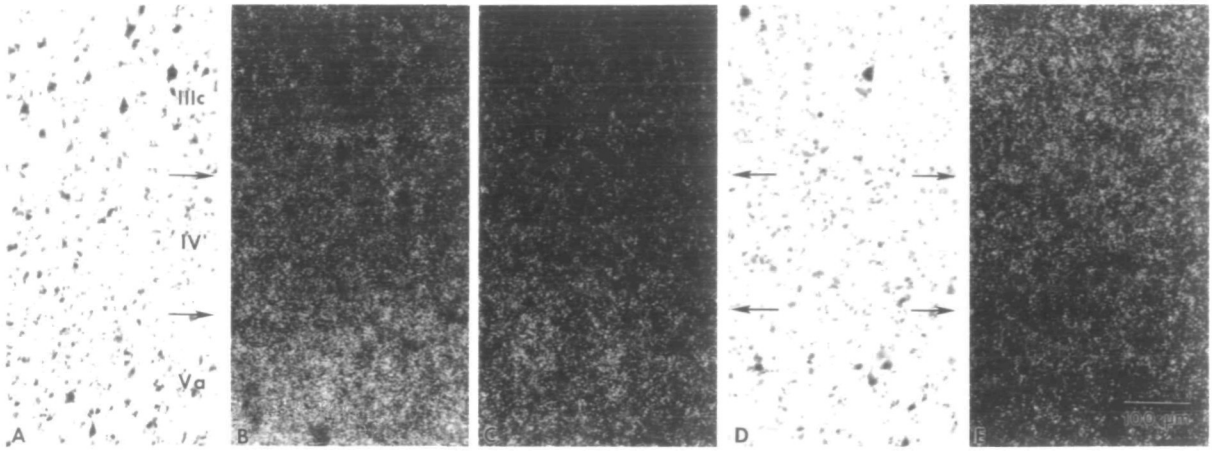

Figure 3. OXO-M/PZ binding in two class 3 cases (*B* and *C*) and their associated neuronal architecture (*A* and *D*, respectively). In the first case, neuron density was low in layer Va and there were high levels of gliosis, while in the second case neuron density was somewhat higher. Binding of OXO-M/PZ in a normal case (*E*) was higher in layers IIIc and IV than it was in layer Va. The autoradiograph in *B* was processed on the same slide as that for the control case in *E*. Therefore, the quantitative differences between these two autoradiographs are particularly significant

possible that OXO-M/PZ binding was related to changes in neuron density, particularly in this layer There was no relationship between OXO-M/PZ binding and neuron density in layer Va in control cases as shown in Figure 4 ($r = 0.33$; $F = 0.87$; $p = 0.38$). There was, however, a highly significant and inverse linear relationship between neuron density and OXO-M/PZ binding in layer Va of class 3 cases ($r = -0.98$; $F = 40\ 2$; $p = 0.024$). Figure 3, *A* and *B*, contains photographs of a class 3 case with high densities of OXO-M/PZ binding, low numbers of layer Va neurons, and relatively high gliosis, and *C* and *D*, of a class 3 case with lower OXO-M/PZ binding, higher numbers of layer Va neurons, and limited gliosis. Although there was no significant relationship between OXO-M/PZ binding and neuron density in layer Va when all DAT cases were considered together, removal of the two class 4 cases uncovered a significant correlation between OXO-M/PZ binding and neuron density in layer Va ($r = -0.76$; $F = 11.2$; $p = 0.01$).

Since class 2 cases had a relatively punctate lesion in layer IIIa,b, the possible relationships between OXO-M/PZ binding and neuron densities were explored in this layer. In control cases there was a positive correlation between these parameters ($r = 0.74$; $F = 8.62$; $p = 0.022$); however, there was not a significant relationship between these parameters in the DAT cases ($r = -0.30$; $F = 1.00$; $p = 0.34$).

AF-DX 116 Binding

The OXO-M/PZ protocol has been used to define presynaptic binding, and it likely reflects the transport of m2 receptors to the axon terminals of basal forebrain and limbic thalamic neurons. Since AF-DX 116 has also been used to label these receptors in experimental animals, AF-DX 116 was used in an attempt to identify binding to m2 receptors in these cases. The distribution of AF-DX 116 binding was assessed with ^{3}H-AF-DX 116 and a 100 nM AF-DX 116 block of OXO-M/PZ binding.

Figure 5 is a graph of ^{3}H-AF-DX 116 and OXO-M/PZ/AF-DX 116 binding in control and class 3 cases ($n = 4$ for each group). The 100 nM unlabeled AF-DX 116 appears to have elevated binding of OXO-M/PZ in most layers of the control cases while not altering binding in the class 3 cases. The difference in OXO-M/PZ binding noted in superficial layers between control and class 3 cases was not present when unlabeled AF-DX 116 was included in the incubation buffer. Furthermore, the layer Va peak in class 3 OXO-M/PZ binding was not altered with 100 nM AF-DX 116.

Table 2
Oxotremorine-M binding

Layer	Control	All DAT	Class 1	Class 2	Class 3	Class 4
Ia	157 ± 18	226 ± 15*	167 ± 12	262 ± 13*	261 ± 22*	189 ± 4
Ic	188 ± 15	238 ± 13*	193 ± 15	281 ± 26*	269 ± 15*	208 ± 3
II	190 ± 11	245 ± 14*	208 ± 6	271 ± 32*	276 ± 16*	197 ± 10
IIIa,b	205 ± 11	240 ± 13	193 ± 5	261 ± 34**	271 ± 11*	219 ± 4
IIIc	240 ± 15	280 ± 16	218 ± 12	332 ± 22*	300 ± 21**	254 ± 30
IV	223 ± 11	292 ± 15*	251 ± 41	304 ± 22*	328 ± 19*	260 ± 5
Va	228 ± 8	347 ± 20*	283 ± 24**	351 ± 4*	423 ± 26*	285 ± 5
Vb	205 ± 9	282 ± 13*	260 ± 34**	293 ± 15*	303 ± 23*	254 ± 26
VI	161 ± 10	214 ± 14*	225 ± 35**	204 ± 26	234 ± 20*	169 ± 40

*$p \leq 0.01$; **$p \leq 0.05$; in comparison to control values.

Downloaded from http://cercor.oxfordjournals.org/ at Boston University on June 28, 2015

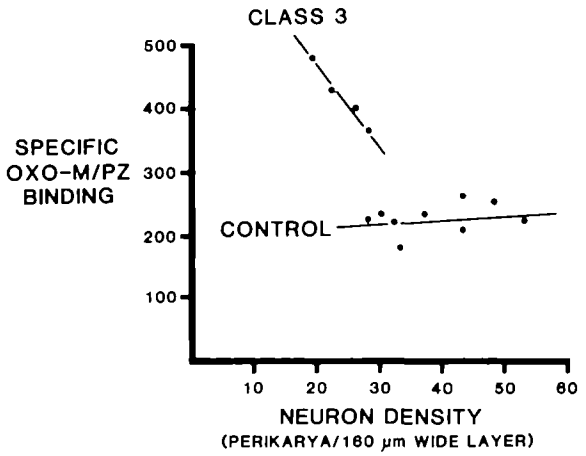

Figure 4. Linear regressions between OXO-M/PZ binding and layer Va neuron densities for control and class 3 DAT cases. There was no significant correlation between these variables for control cases, however, that for class 3 DAT cases was a highly significant and inverse relationship.

In control cases the binding of ^{3}H-AF-DX 116 was higher in superficial layers I–IIIc than it was in deeper layers. There were no differences between the laminar distributions of ^{3}H-AF-DX 116 binding in control and class 3 cases. Nonspecific ^{3}H-AF-DX 116 binding as a percentage of total binding in layer Va of class 3 cases was very high at 70.0 ± 8.9%. Under the incubation parameters employed here, therefore, there appears to have been only limited specific AF-DX 116 binding and it does not appear to compete effectively with OXO-M/PZ binding in human brain.

Discussion

Binding to muscarinic ACh receptors substantially increased in cingulate cortex in particular classes of Alzheimer's disease. Elevated OXO-M/PZ binding may have been associated with m2 receptors because there was no change in pirenzepine binding in these same cases (Vogt et al., 1991), although it was possible that m4 receptors had an increased affinity for oxotremorine-M that was not recognized by pirenzepine. Furthermore, OXO-M/PZ binding was inversely correlated with neuron densities in layer Va and primitive NPs in class 3 cases; that is, cases with highest OXO-M/PZ binding had fewest neurons and primitive NPs. It appears, therefore, that there was a progression of DAT pathology within individual classes of the disease. Finally, although alterations in OXO-M/PZ binding were likely due to changes in binding to m2 receptors, this binding was not sensitive to AF-DX 116.

Muscarinic Receptor Subtypes

One of the principal issues raised by these findings is which muscarinic receptor is altered in DAT and how does its cellular localization account for elevated OXO-M/PZ binding. OXO-M/PZ has been used in experimental animals to localize presynaptic muscarinic receptors (Vogt and Burns, 1988; Vogt et al., 1992) that are likely m2 receptors (Buckley et al., 1988). Since pirenzepine was used in the present experiments to block binding to m1, m3, and m4 receptors and ^{3}H-pirenzepine binding was unaltered in these same cases (Vogt et al., 1991), it is likely that the elevated binding of OXO-M/PZ was associated with m2 receptors. An alternative explanation is that elevated OXO-M/PZ binding is due to increased affinity of m4 receptors for oxotremorine-M as discussed at the end of this section.

Although the present findings do not clarify whether altered OXO-M/PZ binding was the result of increased receptor affinity or density, the laminar distribution of changes in binding can be used to evaluate which circuits are most likely involved. Since m2 receptors are expressed by neurons in the rat basal forebrain and anteroventral thalamic nuclei (Buckley et al., 1988) and neurons in each of these nuclei de-

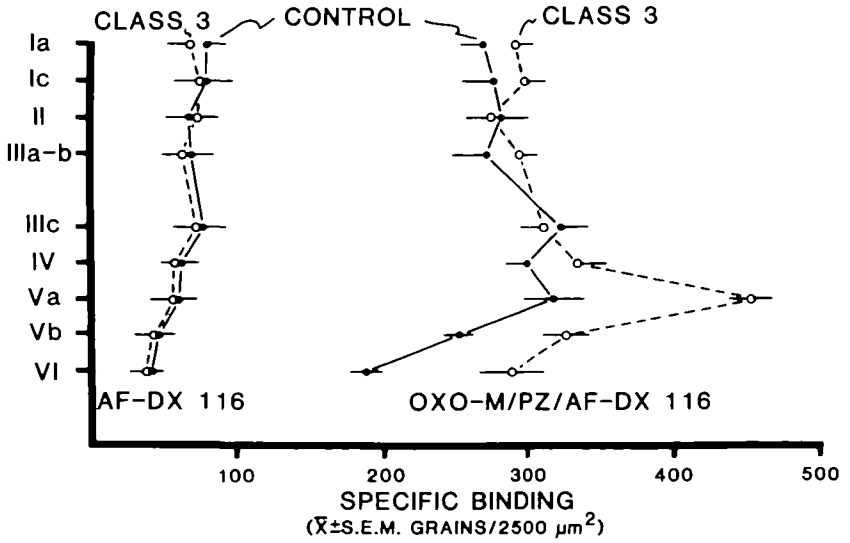

Figure 5. Two methods for assessing AF-DX 116 binding. The laminar distributions on the *left* are grain densities for ^{3}H-AF-DX 116 binding, while those on the *right* are for OXO-M/PZ binding in the presence of 100 μM unlabeled AF-DX 116. In neither instance can the elevation of muscarinic ligand binding in layer Va of class 3 cases be attributed to AF-DX 116–sensitive sites.

Downloaded from http://cercor.oxfordjournals.org/ at Boston University on June 28, 2015

generate in DAT (Whitehouse et al., 1982; Arendt et al., 1983; Braak and Braak, 1991a), it is possible that binding of m2 receptors in either of these afferents to cingulate cortex are altered in DAT. It is unlikely that the changes observed are due to changes in thalamic afferents for the following reasons. First, the anteroventral nucleus in the monkey projects mainly to areas 29 and 30 in the depths of the callosal sulcus (Vogt, 1985), while only the anteromedial nucleus projects to area 23 (Vogt et al., 1987). Second, the rat does not have a medial pulvinar nucleus and so it is not yet known whether or not neurons in this nucleus synthesize m2 receptors. Even if they do, however, this nucleus projects mainly to layers IIIc and IV of area 23 (Baleydier and Mauguiere, 1985), while the greatest increase in OXO-M/PZ binding was in layers IV and Va, and there were moderate increases in layers I–III. In view of the relatively precise laminar termination patterns of thalamic afferents in cingulate cortex and specificity in m2 synthesis in the anteroventral nucleus, it is possible that alterations in binding of the variety observed in the present study are associated with connections that have a diffuse distribution within cingulate cortex.

A likely source of elevated OXO-M/PZ binding in area 23 is sprouting of cholinergic afferents. Rodent studies have shown that posterior cingulate cortex receives basal forebrain input mainly in layers V and VI and less so in superficial layers (Saper, 1984; Luiten et al., 1987). Sprouting of this broadly distributed afferent is suggested by Slotkin et al. (1990), who observed increased choline uptake into synaptosomes of DAT neocortex. Furthermore, although Henke and Lang (1983) reported an overall reduction in ChAT activity in layers II and III of posterior cingulate cortex, there were four of nine cases that had a significant increase in the activity of this enzyme in layers I–IV. Thus, it is possible that sprouting of cholinergic projections to layers I–Va accounts for much of the elevated OXO-M/PZ binding in DAT. The extent to which this sprouting might be associated with changes in binding to choline uptake sites and ChAT activity is worth consideration in future investigations.

An alternative hypothesis for elevated OXO-M/PZ binding is that m4 receptors have an increased affinity for oxotremorine-M and that binding to these receptors is not blocked by pirenzepine. Cortical neurons express m4 receptors (Buckley et al., 1988), and these receptors have a high affinity for oxotremorine (Peralta et al., 1987). Elevated m4 binding could be associated with intact somatodendritic processes and/or sprouting dendrites, since Golgi (Scheibel and Tomiyasu, 1978), electron microscopic (Paula-Barbosa et al., 1980), and tau immunohistochemical (Ihara, 1988) studies have shown dendritic sprouting in DAT neocortex. The present study shows an inverse association between OXO-M/PZ binding and neuron density in layer Va. There was no evidence in the thioflavin S preparations, however, of large numbers of diseased dendrites, and this relationship was not present in layer IIIa,b. Furthermore, there was very high OXO-M/PZ binding in layer IV of class 3 where there were essentially no neurons. Thus, if high-affinity m4 receptors are involved in elevated OXO-M/PZ binding in either intact or sprouting dendrites, these would have to originate from the few remaining neurons in deep layers that have apical dendrites passing through layers IV and Va.

Amyloid Deposition and Neuron Degeneration

β-Amyloid protein is deposited in NPs in DAT (e.g., Selkoe, 1989), and NPs occur throughout the limbic cortices including area 23 (Arnold et al., 1991). In light of the potential neurotoxicity of the β-amyloid peptide (Yankner et al., 1990; Mattson et al., 1992), the relationship between NP deposition and neuron degeneration is worth consideration. The present study shows that there is a wide range of NP densities in cingulate cortex and that there is no correlation between neuron degeneration in layer Va and the total number of NPs for all DAT cases. For class 3 cases, however, there is a positive relationship between primitive NP and neuron densities in layer Va. Thus, cases with fewer neurons in layer Va have fewer NPs, and cases with higher numbers of neurons have more NPs. This implies that, if NP formation is associated with cingulate neuron degeneration in the class 3 cases, as the NPs are elaborated they not only form mature and compact plaques, but some also disappear. These combined processes may account for the wide variation in the densities of NPs in cingulate and other neocortical areas. Furthermore, deposition of β-amyloid protein may account for neuron degeneration in some cases such as those in classes 2 and 3, but not in other cases such as those in class 4.

Disease Progression within a Class

The original proposal to classify DAT cases based on laminar specificities in neuron degeneration (Vogt et al., 1990) appeared to be at odds with earlier studies that suggested a progression in the expression of this disease (Brun and Englund, 1981). Recent studies of amyloid deposition by Braak and Braak (1991b) suggest that retrosplenial cortex (areas 29 and 30) tends to be impacted later in the disease than are hippocampal and entorhinal cortices. In view of the present findings for class 3 cases that neuron degeneration, NPs, and OXO-M/PZ binding are correlated, there is the likelihood that DAT progression occurs within individual classes.

If elevated OXO-M/PZ binding reflects sprouting of cholinergic afferents as suggested above, the following sequence of events may occur in cingulate cortex in class 3 cases. (1) Early, preclinical stages of class 3 may not have cingulate neuron degeneration, little or no β-amyloid protein deposition, and likely no sprouting of cholinergic afferents. (2) As the disease enters clinical levels of expression and hippocampal and parahippocampal cortices develop NPs and NFTs, it is likely that cingulate neurons only in layer IV degenerate and that there are low numbers of immature NPs and modest sprouting of cholinergic axons. (3) As the disease progresses to more severe

Downloaded from http://cercor.oxfordjournals.org/ at Boston University on June 28, 2015

clinical stages, that is, when cases frequently become available for postmortem studies, degeneration of layer IV neurons is severe in cingulate cortex and pyramidal neurons in layer Va degenerate, as do their associated apical dendrites in superficial layers. Gliosis is prominent throughout the cortical thickness, and there is a maturation of NPs and increased proliferation of cholinergic afferents. (4) At the terminal stages of class 3 cases, neuron degeneration in layer Va is severe, NP regression occurs, and cholinergic afferents reach their maximal level of sprouting. It is quite possible that this same sequence of events occurs in parahippocampal areas early in the preclinical stages of the disease.

The extent to which there are interactions among the classes based on neuron degeneration is still not known. Although the classes may represent five independent sets of cases because the age at disease onset and duration of the disease is similar for each class (Vogt et al., 1990), it is also possible that there are some interactions. The two most likely possibilities are that (1) class 1 cases with no neuron degeneration could precede any of the other classes, or (2) class 5 cases with severe and non-laminar-specific degeneration could be the terminal stage of any of the other classes. It is interesting to note, however, that the earliest onset and shortest disease duration occur in the class 5 cases (Vogt et al., 1990).

In conclusion, the classes of DAT pathology in cingulate cortex and the progression of pathology within each lead to new hypotheses about relationships between neuron degeneration, deposition of β-amyloid protein, and sprouting of cholinergic afferents. It is proposed that the progression of DAT pathology in cingulate cortex occurs in other limbic cortical areas, such as entorhinal cortex, in very early and preclinical forms of the disease. Thus, temporal areas could reflect classes of neuron degeneration and disease progression within each, but these processes are not available for study in postmortem cases. Therefore, the expression of borderline neuropathology in cingulate cortex in postmortem cases provides a unique region in which to study DAT.

Notes

We thank the following individuals for their assistance in providing samples of cingulate cortex for these studies Drs. Devay Lathi, Ladislav Volicer, and Chompol Mahasaen at the Veterans Administration Hospital (Bedford, MA); Dr. Edward Bird at the Brain Tissue Resource Center, McLean Hospital (Belmont, MA); Dr. Judith Marquis at Boston University School of Medicine (Boston, MA), Dr. J Ulrich at the Institute für Pathologie der Universität Basel (Basel, Switzerland). This research was supported by NIH-NINDS Grant NS 18745, NIH-NIA Grant AG 11480, the Department of Veterans Affairs, and BRSG funding for the Bowman Gray School of Medicine Brain Resource Center Grant RR 05404.

Correspondence should be addressed to Brent A Vogt, Department of Physiology and Pharmacology, Bowman Gray School of Medicine, Medical Center Boulevard, Winston-Salem, NC 27157-1083.

References

Arendt T, Bigl V, Arendt A, Tennstedt A (1983) Loss of neurons in the nucleus basalis of Meynert in Alzheimer's disease, paralysis agitans and Korsakoff's disease. Acta Neuropathol (Berl) 61:101–108.

Arnold SE, Hyman BT, Flory J, Damasio AR, Van Hoesen GW (1991) The topographical and neuroanatomical distribution of neurofibrillary tangles and neuritic plaques in the cerebral cortex of patients with Alzheimer's disease. Cereb Cortex 1.103–116.

Baleydier C, Mauguiere F (1985) Anatomical evidence for medial pulvinar connections with the posterior cingulate cortex, the retrosplenial area, and the posterior parahippocampal gyrus in monkeys J Comp Neurol 232:219–228.

Braak H, Braak E (1991a) Alzheimer's disease affects limbic nuclei of the thalamus. Acta Neuropathol (Berl) 81:261–268.

Braak H, Braak E (1991b) Neuropathological staging of Alzheimer-related changes. Acta Neuropathol (Berl) 82: 239–259.

Brun A, Englund E (1981) Regional pattern of degeneration in Alzheimer's disease: neuronal loss and histopathological grading Histopathology 5:549–564.

Buckley NJ, Bonner TI, Brann MR (1988) Localization of a family of muscarinic receptor mRNAs in rat brain. J Neurosci 8:4646–4652.

Buckley NJ, Bonner TI, Buckley CM, Brann MR (1989) Antagonist binding properties of five cloned muscarinic receptors expressed in CHO-K1 cells. Mol Pharmacol 35. 469–476

Couch JV (1982) Fundamentals of statistics for the behavioral sciences, pp 266–270 New York: St. Martin's

Danielsson E, Eckernäs S-Å, Westlind-Danielsson A, Nordström Ö, Bartfai T, Gottfries C-G, Wallin A (1988) VIP-sensitive adenylate cyclase, guanylate cyclase, muscarinic receptors, choline acetyltransferase and acetylcholinesterase, in brain tissue afflicted by Alzheimer's disease/senile dementia of the Alzheimer type. Neurobiol Aging 9.153–162.

Dörje F, Wess J, Lambrecht G, Tacke R, Mutschler E, Brann MR (1991) Antagonist binding profiles of five cloned human muscarinic receptor subtypes. J Pharmacol Exp Ther 256:727–733.

Giacobini E, DeSarno P, Clark B, McIlhany M (1989) The cholinergic receptor system of the human brain: neurochemical and pharmacological aspects in aging and Alzheimer. Prog Brain Res 79:335–342.

Henke H, Lang W (1983) Cholinergic enzymes in neocortex, hippocampus, and basal forebrain of non-neurological and senile dementia of Alzheimer-type patients. Brain Res 267:281–291

Ihara Y (1988) Massive somatodendritic sprouting of cortical neurons in Alzheimer's disease. Brain Res 459:138–144.

Luiten PGM, Gaykema RPA, Traber J, Spencer DG Jr (1987) Cortical projection patterns of magnocellular basal nucleus subdivisions as revealed by anterogradely transported *Phaseolus vulgaris* leucoagglutinin. Brain Res 413: 229–250.

Mash DC, Flynn DD, Potter LT (1985) Loss of M2 muscarinic receptors in the cerebral cortex in Alzheimer's disease and experimental cholinergic denervation Science 228:1115–1117.

Mattson MP, Cheng B, Davis B, Bryant K, Lieberburg I, Rydel RE (1992) β-Amyloid peptides destabilize calcium homeostasis and render human cortical neurons vulnerable to excitotoxicity. J Neurosci 12:376–389

McKhann G, Drachmann D, Folstein D, Katzmann R, Price D, Stadlin EM (1984) Clinical diagnosis of Alzheimer's disease: report of the NINCDS-ADRDA work group under the auspices of the Department of Health and Human Services Task Force on Alzheimer's disease. Neurology 34:939–944

Nordberg A, Winblad B (1986) Reduced number of [^{3}H]nicotine and [^{3}H]acetylcholine binding sites in the frontal cortex of Alzheimer brains Neurosci Lett 72:115–119

Downloaded from http://cercor.oxfordjournals.org/ at Boston University on June 28, 2015

Paula-Barbosa MM, Cardoso RM, Guimaraes MI, Cruz C (1980) Dendritic degeneration and regrowth in the cerebral cortex of patients with Alzheimer's disease. J Neurol Sci 45:129–134.

Pearson RCA, Sofroniew MV, Cuello AC, Powell TPS, Eckenstein F, Esiri MM, Wilcock GK (1983) Persistence of cholinergic neurons in the basal nucleus in a brain with senile dementia of the Alzheimer's type demonstrated by immunohistochemical staining for choline acetyltransferase Brain Res 289.375–379.

Peralta EG, Ashkenazi A, Winslow JW, Smith DH, Ramachandran J, Capon DJ (1987) Direct primary structures, ligand-binding properties and tissue-specific expression of four human muscarinic acetylcholine receptors. EMBO J 6:3923–3929.

Procter AW, Lowe SL, Palmer AM, Francis PT, Esiri MM, Stratmann GC, Najlerahim A, Patel AJ, Hunt A, Bowen DM (1988) Topographical distribution of neurochemical changes in Alzheimer's disease. J Neurol Sci 84.125–140

Rossor MN, Garrett NJ, Johnson AL, Mountjoy CQ, Roth M, Iversen LL (1982) A post-mortem study of the cholinergic and GABA systems in senile dementia. Brain 105·313–330.

Saper CB (1984) Organization of cerebral cortical afferent systems in the rat· II. Magnocellular basal nucleus. J Comp Neurol 222 313–342.

Scheibel AB, Tomiyasu U (1978) Dendritic sprouting in Alzheimer's presenile dementia. Exp Neurol 60·1–8

Schwartz PH, Kurucz J, Kurucz A (1964) Recent observations on senile cerebral changes and their pathogenesis J Am Geriatr Soc 12:908–922

Selkoe DJ (1989) Biochemistry of altered brain proteins in Alzheimer's disease. Annu Rev Neurosci 12·463–490.

Slotkin TA, Seidler FJ, Crain BJ, Bell JM, Bissette G, Nemeroff CB (1990) Regulatory changes in presynaptic cholinergic function assessed in rapid autopsy material from patients with Alzheimer's disease. implications for etiology and therapy Proc Natl Acad Sci USA 87:2452–2455.

Vogt BA (1985) Cingulate cortex. In: Cerebral cortex, Vol 4 (Peters A, Jones EG, eds), pp 89–149. New York: Plenum.

Vogt BA, Burns DL (1988) Experimental localization of muscarinic receptor subtypes to cingulate cortical afferents and neurons. J Neurosci 8:643–652.

Vogt BA, Pandya DN, Rosene DL (1987) Cingulate cortex of the rhesus monkey: I. Cytoarchitecture and thalamic afferents. J Comp Neurol 262:256–270.

Vogt BA, Van Hoesen GW, Vogt LJ (1990) Laminar distribution of neuron degeneration in posterior cingulate cortex in Alzheimer's disease. Acta Neuropathol (Berl) 80. 581–589.

Vogt BA, Crino PB, Volicer L (1991) Laminar alterations in gamma-aminobutyric acid$_A$, muscarinic, and β adrenoceptors and neuron degeneration in cingulate cortex in Alzheimer's disease. J Neurochem 57:282–290.

Vogt BA, Crino PB, Jensen EL (1992) Multiple heteroreceptors on limbic thalamic axons· M2 acetylcholine, serotonin 1B, β_2-adrenoceptors, μ-opioid, and neurotensin Synapse 10·44–53.

Yankner BA, Duffy LK, Kirschner DA (1990) Neurotrophic and neurotoxic effects of amyloid β protein· reversal by tachykinin neuropeptides. Science 250:279–282.

Young WS III, Kuhar MJ (1979) A new method for receptor autoradiography ^{3}H-opioid receptor labeling in mounted tissue sections. Brain Res 179:255–270

Whitehouse PJ, Price DL, Struble RG, Clark AW, Coyle JT, DeLong MR (1982) Alzheimer's disease and senile dementia: loss of neurons in the basal forebrain. Science 215:1237–1239.

Wisniewski HM, Terry RD (1973) Reexamination of the pathogenesis of the senile plaque. Prog Neuropathol 2.1–26.

Downloaded from http://cercor.oxfordjournals.org/ at Boston University on June 28, 2015